

Responses to Reviewers

Reviewer 2

The manuscript reported an improved CRM method to measure OH reactivity. The reactor of traditional CRM method was modified to suppress HO₂ formation. The lab experiment results were promising that the measured and calculated k_{OH} by trace gases have good linearity. The ambient measurements showed that the new ICRM method could be used under urban ambient air. The manuscript is well within the scope of AMT. I recommend publication after attention to the following comments.

Reply: We are very grateful for all the detailed comments and the valuable suggestions, which helped us greatly in improving our manuscript. Please find the response to individual comments below.

General comments:

1. The reaction time of NO+HO₂ (or OH) in arm A should be clearly specified. HONO will be formed with no doubt and will it cause any interference with CRM?

Reply: (1) The initial HO₂ concentration is about 4 ppbv. The lifetime of HO₂ at 50 ppbv NO is at the time scale of 0.1 s, given that the reaction rate constant of NO+HO₂ is $8.0 \times 10^{-12} \text{ cm}^3 \text{ molecule}^{-1} \text{ s}^{-1}$. The reaction time of NO+HO₂ in arm A is estimated to be around ~ 0.1 s, during which most of HO₂ will be consumed. Hence there will be only a small fraction of HO₂ entering the main body of the reactor. (2) In the reactor, OH reacts with introduced or ambient NO to produce HONO, which can reproduce OH and NO by photolysis. As we have improved the structure of arm A to avoid UV light entering the main body of reactor, the photolysis of HONO is expected to be negligible. We pointed this out in line 478-480 of the revised manuscript: “**The change of the structure of arm A also ensures that the photolysis of H₂O, HONO, NO₂, and VOCs inside the ICRM reactor is weaker than that in the original CRM system.**”

We added the following sentences in the revised manuscript (Line 451-456): **Finally, the reaction time between HO₂ and NO should be noted. The initial HO₂ concentration is about 4 ppbv. The lifetime of HO₂ at 50 ppbv NO is at the time**

30 **scale of 0.1 s, given that the reaction rate constant of NO+HO₂ is 8.1×10⁻¹² cm³**
31 **molecule⁻¹ s⁻¹ (Sander, 2006). The reaction time of NO+HO₂ in arm A is estimated**
32 **to be around 0.1 s, during which most of HO₂ will be consumed. Hence there will**
33 **be only a small fraction of HO₂ entering the main body of the reactor.**

34 We added the following sentences in the revised manuscript (Line 481-484): **In**
35 **this system, OH reacts with introduced NO or ambient NO to produce HONO,**
36 **which can reproduce OH and NO by photolysis. As we have improved the**
37 **structure of arm A to avoid UV light entering main body of the reactor, photolysis**
38 **of HONO is expected to be low.**

39

40 2. In section 3.1, the NO addition measurement showed that Pyrrole concentration
41 decreased to the minimum with NO around 40 ~ 50 ppbv (Fig.2). I think the increase
42 of Pyrrole with NO is due to NO+OH reaction which lower the produced OH
43 concentration.

44 Reply: Yes, we agree with you that the increase of pyrrole with NO is due to
45 NO+OH reaction which lower the produced OH concentration.

46 Line 273-274: **As the NO concentration exceeds 50 ppbv, pyrrole**
47 **concentrations increase again, due to large excess NO competes with pyrrole for**
48 **reaction with OH radicals.**

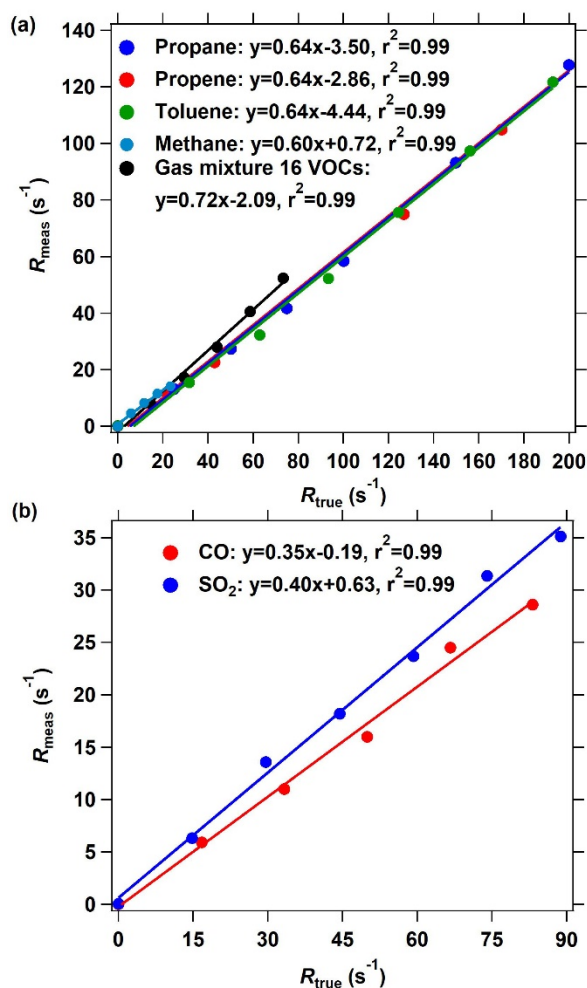
49

50 3. In section 3.2 and Fig.4, the authors gave very promising dataset of the measured
51 and calculated k_{OH}. The linearity were all very good but the slope were not close to 1.
52 Since the ICRM method introduced extra NO in the reactor, the cycling of OH-HO₂-
53 OH can not be avoid due to the reaction time in the reactor. The influence of initial
54 HO₂ was suppressed and at mean time the HO_x cycling was enhanced. I would guess
55 the slopes of CO and VOCs in Fig. 4 are related to this issue. Probably more VOCs
56 should be tested before application in ambient air.

57 Reply: Yes, as the ICRM method introduced extra NO in the reactor, the cycling
58 of OH-HO₂-OH cannot be avoid due to the reaction time (~11s) in the reactor, and the

59 recycled OH from RO₂ will deplete pyrrole thus leading to a R_{meas} lower than the R_{true} .
60 We agree with the reviewer that the slopes of CO and VOCs lower than one in Fig. 4
61 are related to this issue. We also calibrate methane in the revised manuscript and similar
62 results are shown (Figure 4a). In addition to the four individual VOC species, we also
63 calibrated the mixed standard gases with 16 VOC species. The calibration slope is close
64 to those of the three individual VOC species, indicating that the RO₂ + NO reactions
65 for these investigated VOCs are similar. Nevertheless, we agree with the reviewer that
66 it is necessary to calibrate more VOC species in the future, especially considering that
67 different VOCs species dominate in different environment, such as forest areas and
68 various emission sources. For example, isoprene and terpenes have high reactivity
69 contribution in forests and rural sites. Therefore, isoprene, α -Pinene and β -Pinene is
70 suggested to be calibrated in the following study. Typical branched olefin, other
71 aromatics (such as ethylbenzene) and important oxygenated VOCs (such as
72 formaldehyde and glyoxal) should also be calibrated in the future.

73 We added the following sentences in the revised manuscript (Line 404-414): **In**
74 **this study, we calibrated four individual representative VOC species (methane,**
75 **propane, propene, toluene). In addition, we also calibrated the mixed standard**
76 **gases with 16 VOC species including representative oxygenated VOCs**
77 **(acetaldehyde, methanol, ethanol, acetone, acetonitrile, methyl vinyl ketone,**
78 **methyl ethyl ketone), biogenic VOCs (isoprene, α -pinene), typical aromatics**
79 **(benzene, toluene, o-xylene, 1,2,4-trimethylbenzene, naphthalene, phenol, m-**
80 **cresol). The calibration slope is close to those of the four individual VOC species,**
81 **indicating that the RO₂ + NO reactions for these investigated VOCs should be**
82 **similar. Nevertheless, given that there are different VOCs compositions in**
83 **different environment such as forest, urban area and emission sources,**
84 **calibrations for more individual VOCs species might be also needed.**



85
 86 Figure 4. The OH reactivity calibration of the improved CRM system using different
 87 standard gases. (a) The calibrating results of organic species including methane,
 88 propane, propene, toluene, and mixture gases of 16 VOC species through arm C. (b)
 89 The calibrating results of inorganic species including CO and SO₂. The measured OH
 90 reactivity was calculated based on the C2 mode shown in Fig. 2 in the ICRM system.

91
 92 Specific comments:

93 Line 58: Better to include NO in the equation.

94 Reply: We thank the reviewer for the careful comment. We have modified
 95 equation 1 in the revised manuscript (Line 58):

$$96 R_{OH} = k_{CO}[CO] + k_{NO}[NO] + k_{NO_2}[NO_2] + k_{SO_2}[SO_2] + k_{O_3}[O_3] + \sum_i^n k_{VOC_i}[VOC_i] \quad (1)$$

97
 98 Line 131: Please specify the brand and type of the lamp, as well as its emission line.

99 Reply: The brand and type of UV lamp that we used is Analytik Jean (type: 90-
100 0012-01), and its emission line is 254 nm.

101 We added the following sentences in the revised manuscript (Line 132): **Arm A**
102 **consists of a pen-ray spectral mercury lamp (Analytik Jean; 90-0012-01), over**
103 **which nitrogen (humidified or dry) is passed through arm B at a constant flow**
104 **rate.**

105 Line 158: “An underlying assumption of the CRM approach is that the influence of the
106 species in ambient air on OH radicals in the reactor is ignorable.” The sentence is
107 ambiguous. It is also useful to give the theoretical OH mixing ratio in the reactor here.

108 Reply: We thank the reviewer for the comment. The species in ambient air will of
109 course influence the concentration of OH radicals by reacting with OH radicals. We
110 mean that an underlying assumption of the CRM approach is that the production of OH
111 radicals is just from the photolysis of H₂O under UV lamp, and the influence of the
112 species in ambient air on the production of OH radicals in the reactor is ignorable. The
113 theoretical OH mixing ratio in the original reactor is about 5 ~ 20 ppbv, which depends
114 on the introduced pyrrole concentration to ensure the pyrrole/OH ratio is 2:1~3:1. For
115 ICRM, the total OH radical concentration including production from UV lamp and from
116 the reaction of HO₂ with NO is about 10 ppbv.

117 We added the following sentences in the revised manuscript (Line 160-164): **An**
118 **underlying assumption of the CRM approach is that the influence of the species in**
119 **ambient air on the production of OH radicals in the reactor is ignorable. The**
120 **theoretical OH mixing ratio in the original CRM reactor is about 5 ~ 20 ppbv,**
121 **which depends on the introduced pyrrole concentration to ensure the Pyrrole/OH**
122 **ratio is 2:1~3:1.**

123 We added also the following sentences in the revised manuscript (Line 284-287):
124 **Under this optimized condition, the pyrrole concentration decreased to 12.3 ppbv,**
125 **indicating the total OH radical concentration including production from UV lamp**
126 **and from the reaction of HO₂ with NO is about 10 ppbv in the ICRM system.**

127

128 Line 181: Did the author try different structure (length, ID. etc) of arm A to get an
129 optimal setup?

130 Reply: (1) The length of arm A will determine initial OH concentration passing
131 into the reactor and the reaction time of HO₂ with NO. The longer arm A is beneficial
132 for longer reaction time of HO₂ with NO, but lower OH concentrations passing into the
133 reactor due to wall loss. We chose an appropriate length of arm A (12 cm) to ensure
134 appropriate OH concentration (4 ppbv) and reaction time of HO₂ with NO (~0.1 s). (2)
135 For ID, arm A consists of two sections of glass tube with 1/2 inch OD (ID: 0.62 cm,
136 length: 7 cm) and one 1/4 inch OD (ID: 0.32 cm, length: 5 cm) respectively. This ensure
137 that UV light is mostly confined in 1/2 inch OD glass tube of arm A, as the glass tube
138 is constructed with decreasing diameter following the direction of gas flow. However,
139 the reaction time of HO₂ with NO in arm A is very short (~0.1 s), which needs to be
140 solved in the future.

141 We modified the following sentences in the revised manuscript (Line 182-193):
142 **Arm A consists of one 1/2 inch OD (ID: 0.62 cm, length: 7 cm) glass tube and one**
143 **1/4 inch OD (ID: 0.32 cm, length: 5 cm) glass tube. The longer arm A is beneficial**
144 **for longer reaction time of HO₂ with NO, but lower OH concentrations passing**
145 **into the reactor due to wall loss. We chose an appropriate length of arm A (12 cm)**
146 **to ensure appropriate OH concentration (4 ppbv) and reaction time of HO₂ with**
147 **NO (~ 0.1 s). The purpose of the two-section structure is to ensure that the UV light**
148 **is mostly confined within a 1/2 inch OD glass tube of arm A, as the diameter of**
149 **arm A goes from wide to slender. The new structure of arm A leads to lower OH**
150 **concentrations (decreased by approximately 50%) passing into reactor compared**
151 **with the original CRM system due to wall loss, but OH radicals produced from the**
152 **reaction of HO₂ radicals with NO can partially compensate for this loss.**

153 We added the following sentences in the revised manuscript (Line 468-475): **Arm**
154 **A consists of two section of glass tube with 1/2 inch OD and 1/4 inch OD,**
155 **respectively (Fig. 1c). UV light is mostly confined in 1/2 inch OD glass tube of arm**
156 **A, as the glass tube is constructed with decreasing diameter following the direction**

157 **of gas flow. This reduces the amount of UV light getting into the main reaction**
158 **part of the reactor. The improved structure of arm A leads to lower OH**
159 **concentrations (decreased by approximately 50%) passing into reactor due to wall**
160 **loss, but the OH radicals produced from the reaction of HO₂ radicals with NO can**
161 **partially compensate for this loss.**

162

163 Line 250: It is better to include OH+NO reaction here. Is this reaction also include in
164 the box model?

165 Reply: Thank you for pointing this out. We have included it. Yes, this reaction
166 was included in the box model for the simulation.

167 Line 263: $NO + OH \rightarrow HONO$ R8

168

169 Line 283: the rate constant of OH+NO should be given here or in Fig.3, when calculated
170 R-true of NO.

171 Reply: Corrected. We have added the reaction rate constant of OH+NO (Line 297).

172 We modified the following sentences in the revised manuscript (Line 297-298):
173 **Measured OH reactivity of NO ($k_{NO} = 9.7 \times 10^{-12} \text{ cm}^3 \text{ molecule}^{-1} \text{ s}^{-1}$ according to**
174 **IUPAC lasted evaluation in November 2017) agreed well with the corresponding**
175 **true values.**

176

177 Line 404: The rate constant were quoted from Atkinson 2004, which is a well-known
178 reference. I would suggest the authors also check the new evaluations or
179 recommendations on JPL-2015 or IPUAC sources.

180 Reply: Thank you for providing us with the useful reference. We have updated the
181 calculated reactivity data by using reaction coefficients from IUPAC sources
182 (<http://iupac.pole-ether.fr>). For reactions that are unavailable in IUPAC, we used
183 reaction coefficients from JPL-2015 evaluation.

184

185 **Other modifications:**

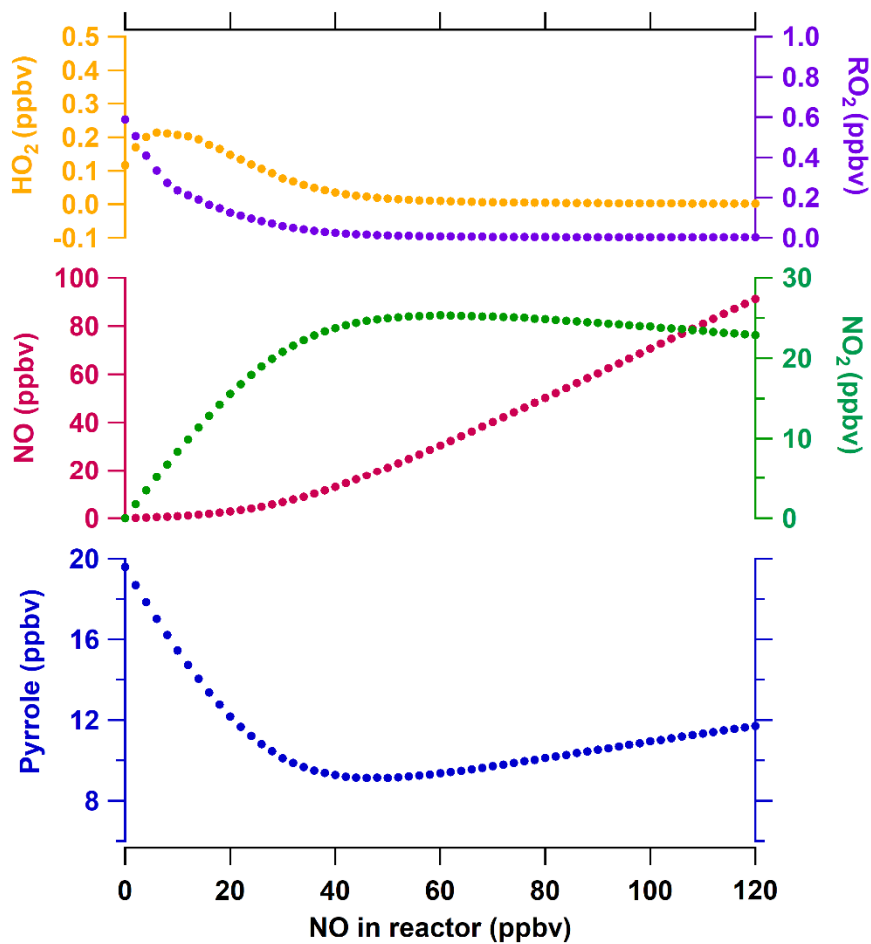
186 (1) Additionally, we added the detection limit in the revised manuscript.

187 Line 535-538: **The detection limit of ICRM was determined to be 2.3 s⁻¹ for an**
188 **averaged pyrrole-to-OH ratio of 2.3 according to the method proposed by**
189 **Michoud et al. (2015) (Fig S9). This means that the minimum detection limit for**
190 **the reactivity of sample air would be about 5 s⁻¹ (typically diluted in the glass**
191 **reactor by a factor 2).**

192 (2) We revised the fitting results between R_{true} and R'_{meas} ($R_{\text{true}} - R'_{\text{meas}}$) increases with
193 NO concentrations for different VOC species and different reactivity levels (Fig. 5 and
194 Line 354-356 in the revised manuscript).

195 Line 355-357: **Similar to previous study (Michoud et al., 2015; Praplan et al.,**
196 **2017; Yang et al., 2017), the difference between R_{true} and R'_{meas} ($R_{\text{true}} - R'_{\text{meas}}$)**
197 **increases with NO concentrations for different VOC species and different**
198 **reactivity levels.**

199 (3) In Figure S2, the solid line is replaced by dots, which is more reasonable for the
200 expression of this Figure.

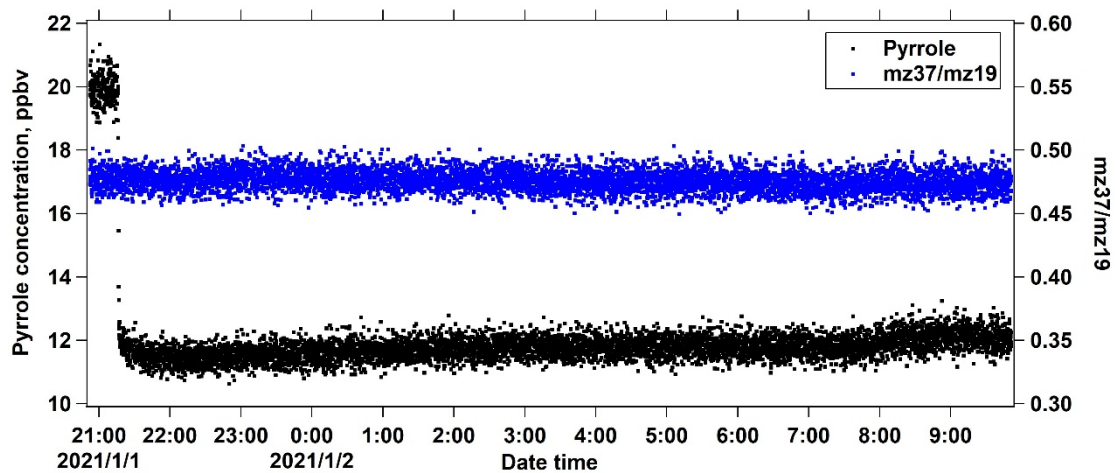


201

202 **Figure S2.** The remaining concentrations of pyrrole, NO, NO₂, HO₂, and RO₂

203 outflowing of the reactor (with the reaction time of ~ 11 s) as a function of introduced

204 NO in the reactor.



205

206

Figure S9. Total OH reactivity detection limit measured for the ICRM.

207 **References**

208 Michoud, V., Hansen, R. F., Locoge, N., Stevens, P. S., and Dusanter, S.: Detailed
209 characterizations of the new Mines Douai comparative reactivity method
210 instrument via laboratory experiments and modeling, *Atmospheric Measurement*
211 *Techniques*, 8, 3537-3553, doi: 10.5194/amt-8-3537-2015, 2015.

212 Praplan, A. P., Pfannerstill, E. Y., Williams, J., and Hellén, H.: OH reactivity of the
213 urban air in Helsinki, Finland, during winter, *Atmospheric Environment*, 169,
214 150-161, doi: 10.1016/j.atmosenv.2017.09.013, 2017.

215 Sander, S. P., B. J. Finlayson-Pitts, R. R. Friedl, D. M. Golden, R. E. Huie, H. Keller-
216 Rudek, C. E. Kolb, M. J. Kurylo, M. J. Molina, G. K. Moortgat, V. L. Orkin, A.
217 R. Ravishankara and P. H. Wine: *Chemical Kinetics and Photochemical Data for*
218 *Use in Atmospheric Studies Evaluation Number 15*, JPL Publication 06-2, Jet
219 *Propulsion Laboratory*, 2006.

220 Yang, Y., Shao, M., Keßel, S., Li, Y., Lu, K., Lu, S., Williams, J., Zhang, Y., Zeng, L.,
221 Nölscher, A. C., Wu, Y., Wang, X., and Zheng, J.: How the OH reactivity affects
222 the ozone production efficiency: case studies in Beijing and Heshan, China,
223 *Atmospheric Chemistry and Physics*, 17, 7127-7142, doi: 10.5194/acp-17-7127-
224 2017, 2017.

225